Electronic Supplementary Material (ESI) for Chemical Communications.

Combining dithieno[3,2-*f*:2',3'-*h*]quinoxaline-based terpolymer and ternary strategies enabling high-efficiency organic solar cells

Sungwoo Jung,[1] Seonghun Jeong,[1] Jiyeon Oh,[1] Seoyoung Kim,[1] Seunglok Lee,[1] Seong-Jun Yoon,[1] and Changduk Yang[1,2]**

[1]School of Energy and Chemical Engineering, Perovtronics Research Center, Low Dimensional Carbon Materials Center, Ulsan National Institute of Science and Technology (UNIST), 50 UNIST-gil, Ulju-gun, Ulsan 44919, South Korea.

[2]Graduate School of Carbon Neutrality, Ulsan National Institute of Science and Technology (UNIST), 50 UNIST-gil, Ulju-gun, Ulsan 44919, South Korea.

E-mail: yang@unist.ac.kr (C.Y.), yoonsj@unist.ac.kr (S.-J.Y.)

Experimental Section

***Materials and Instruments**:* The chemicals and reagents were purchased from Sigma-Aldrich, Alfa Aesar chemical company, and Tokyo Chemical Industry Co., Ltd. without any further purification. All solvents were ACS grade unless otherwise noted. The monomers BDT-F (**1**) & BDD (**2**) were purchased from SunaTech Inc. The co-monomer Qx (**3**) was synthesized according to the previously reported synthetic routes.[1] $Pd_2(dba)_3$ was purchased from Sigma-Aldrich, and P(*o*-Tol)$_3$ was purchased from Alfa Aesar. The molecular weights of the random polymers were characterized with high-temperature gel permeation chromatography (HR-GPC) at 100 °C using polystyrene as the standard in 1,2,4-trichlorobenzene (HPLC grade). UV–Vis absorption spectra in solution and thin films were measured using a UV-1800 (SHIMADZU). Cyclic voltammetry (CV) measurements were performed on an Iviumstat.h with a three-electrode cell system in a nitrogen bubbled 0.1 M *n*-Bu_4NPF_6 solution in acetonitrile at a scan rate of 100 mV s^{-1} at room temperature. An Ag/Ag^+ electrode, platinum wire, and platinum were used as the reference electrode, counter electrode, and working electrode, respectively. The Ag/Ag^+ reference electrode was calibrated using a ferrocene/ferrocenium redox couple as an external standard, whose oxidation potential is set at −4.8 eV with respect to a zero-vacuum level. The HOMO energy levels were obtained from the equation HOMO (eV) = $-(E_{ox}^{onset} - E_{1/2}^{ferrocene} + 4.8)$. The LUMO levels were obtained from the equation LUMO (eV) = $-4.8 - (E_{red}^{onset} - E_{1/2}^{ferrocene})$.

Material Synthesis and Characterization:

Polymerization procedures

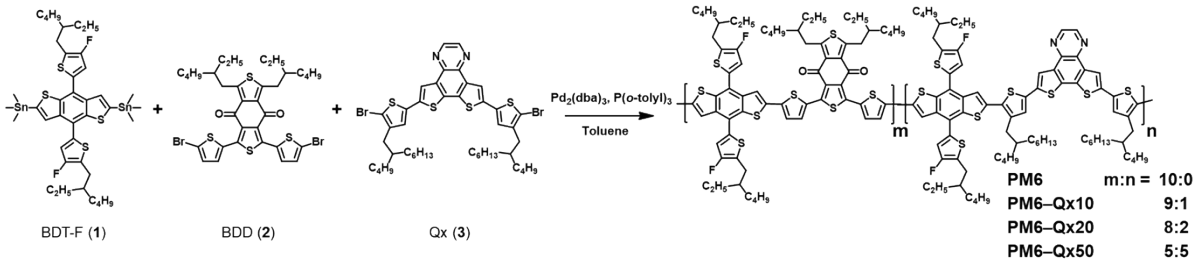

Synthesis of PM6: To a long Schlenk flask, monomer **1** (123 mg, 0.130 mmol), monomer **2** (100 mg, 0.130 mmol), $Pd_2(dba)_3$ (3.6 mg, 0.004 mmol), and P(*o*-tolyl)$_3$ (11.9 mg, 0.04 mmol) were dissolved in freshly distilled toluene (5 mL), and purged with argon for 20 min. The reaction mixture was stirred at 120 °C for 30 min and precipitated to methanol. The crude copolymer was purified using sequential Soxhlet extraction with methanol, acetone, hexane, and chloroform. The chloroform fraction was concentrated and precipitated into methanol. The resulting copolymer was collected using a membrane filter and dried under a high-vacuum oven. Yield 91% (product 145 mg); M_n =38.1 kDa, PDI = 3.22. ^{1}H NMR (600 MHz, $CDCl_3$), δ (ppm): 7.99–6.49 (br), 3.53–2.63 (br), 2.17–1.26 (br), 1.23–0.69 (br).

Synthesis of terpolymer PM6-Qx10: To a long Schlenk flask, monomer **1** (104 mg, 0.111 mmol), monomer **2** (77 mg, 0.100 mmol), co-monomer **3** (10 mg, 0.011mmol), $Pd_2(dba)_3$ (3.0 mg, 0.003 mmol), and P(*o*-tolyl)$_3$ (10.1 mg, 0.033 mmol) were dissolved in freshly distilled toluene (5 mL), and purged with argon for 20 min. The reaction mixture was stirred at 120 °C for 30 min and precipitated to methanol. The crude terpolymer was purified using sequential Soxhlet extraction with methanol, acetone, hexane, and chloroform. The chloroform fraction was concentrated and precipitated into methanol. The resulting terpolymer was collected using a membrane filter and dried under a high-vacuum oven. Yield 92% (product 126 mg); M_n = 39.2 kDa, PDI = 2.98. ^{1}H NMR (600 MHz, $CDCl_3$), δ (ppm): 8.95–8.80 (br), 7.99–6.49 (br), 3.53–2.63 (br), 2.17–1.26 (br), 1.23–0.69 (br).

Synthesis of terpolymer PM6-Qx20: Based on the procedure described above, monomer **1** (104 mg, 0.111 mmol), monomer **2** (68 mg, 0.089 mmol), co-monomer **3** (20 mg, 0.022 mmol) were used for terpolymerization. Yield 92% (product 127 mg); M_n = 39.3 kDa, PDI = 2.81. ^{1}H NMR (600 MHz, $CDCl_3$), δ (ppm): 8.95–8.80 (br), 7.99–6.49 (br), 3.53–2.63 (br), 2.17–1.26 (br), 1.23–0.69 (br).

Synthesis of terpolymer PM6-Qx50: Based on the procedure described above, monomer **1** (104 mg, 0.111 mmol), monomer **2** (43 mg, 0.055 mmol), co-monomer **3** (50 mg, 0.055 mmol) were used for terpolymerization. Yield 87% (product 125 mg); M_n = 39.6 kDa, PDI = 2.44. ^{1}H NMR (600 MHz, $CDCl_3$), δ (ppm): 8.95–8.80 (br), 7.99–6.49 (br), 3.53–2.63 (br), 2.17–1.26 (br), 1.23–0.69 (br).

Device fabrication and Characterization: The patterned ITO-coated glass substrates were rinsed using detergent, acetone and isopropanol and were subsequently dried overnight in an oven. The PSCs were fabricated with a configuration of ITO/PEDOT:PSS/photoactive layer/PDINO/Al, where ITO, PEDOT:PSS, and PDINO refer to indium tin oxide, poly(3,4-ethylenedioxythiophene):poly(styrene sulfonate), and perylenediimide functionalized with amino N-oxide, respectively. PEDOT:PSS (Bayer Baytron4083) was spin-coated at 4000 rpm onto the ITO substrate, followed by annealing at 150 °C for 20 min in air. PDINO was selected as the cathode interlayer to lower the work function of Al.[2] In all cases, the optimal donor-to-acceptor ratio was 1:1.2 (w/w) in a chloroform solvent containing 0.5 vol% 1-chloronaphthalene as a solvent additive and total concentrations of 17.6 and 15.0 mg mL^{-1} for PM6:N3 and PM6-Qx terpolymers:N3 blends, respectively. The solutions were spin-coated onto the PEDOT:PSS layer with a thickness of 100 nm, and the active blend films were annealed at the optimized temperatures (90 °C, 5 min). Then methanol solution of PDINO (1.0 mg ml^{-1}) was then deposited onto the active layer with a spin rate of 3000 rpm for 30 s. Finally, 100 nm aluminum was vacuum deposited under vacuum (<3.0 × 10^{-6} Pa). The active area of each sample was 4.77 mm^2. The current density versus voltage (*J*–*V*) characteristics were recorded using a Keithley 2400 source under the illumination of an AM 1.5G solar simulator with an intensity of 100 mW cm^{-2}. The external quantum efficiency (EQE) measurements were conducted using Model QEX7 by PV measurements Inc. (Boulder, Colorado) in ambient air. The thickness of the active layers was measured using a stylus profilometer (P6, KLA Tencor). The hole and electron mobilities were measured by using the space-charge limited current (SCLC) method. Device structures are ITO/PEDOT:PSS/photoactive layer/Au for hole-only devices and ITO/ZnO/photoactive layer/PDINO/Al for electron-only devices, respectively. The SCLC mobilities were calculated using the Mott-Gurney equation, $J = 9\varepsilon_r\varepsilon_0\mu V^2/8L^3$, where ε_r is the relative dielectric constant

of the organic semiconductor, ε_0 is the permittivity of empty space, m is the mobility of zero-field, L is the thickness of the active layer, and $V = V_{applied} - V_{built\text{-}in} - V_{series\text{-}resistance}$ (the V_{bi} values are 0.2 V and 0 V for the hole-only and the electron-only devices, respectively), where $V_{applied}$ is the voltage applied, and $V_{built\text{-}in}$ is the built-in voltage from the relative work function difference between the two electrodes. $V_{series\text{-}resistance}$ is the voltage caused by the series and contact resistance potential drop ($V_{series\text{-}resistance} = J \times R_{series\text{-}resistance}$). For convenience, the voltage drops caused by this resistance ($R_{series\text{-}resistance}$) were ignored.

Morphology Characterization: AFM images of thin films were obtained using multimode V microscope (Veeco, USA) with a nanoscope controller using Si tips (Bruker). GIWAXS was carried out at the PLS-II 6D U-SAXS and 9A beamline of the Pohang Accelerator Laboratory in Korea. The scattering signal was recorded using a 2-D CCD detector (Rayonix SX165). The X-ray light had an energy of 11.24 KeV. The incidence angle of X-rays was adjusted to 0.09-0.12 to maximize the signal to background ratio.

Calculation of Surface Energy and Interfacial Energy: The surface energy was calculated via measuring the contact angles of two different solvents, distilled water (DI) and diiodomethane (DM) on each film. The surface energy of film was calculated via the Owens–Wendt model and the interfacial energy between each component was estimated via Wu model.

Supplementary Figures

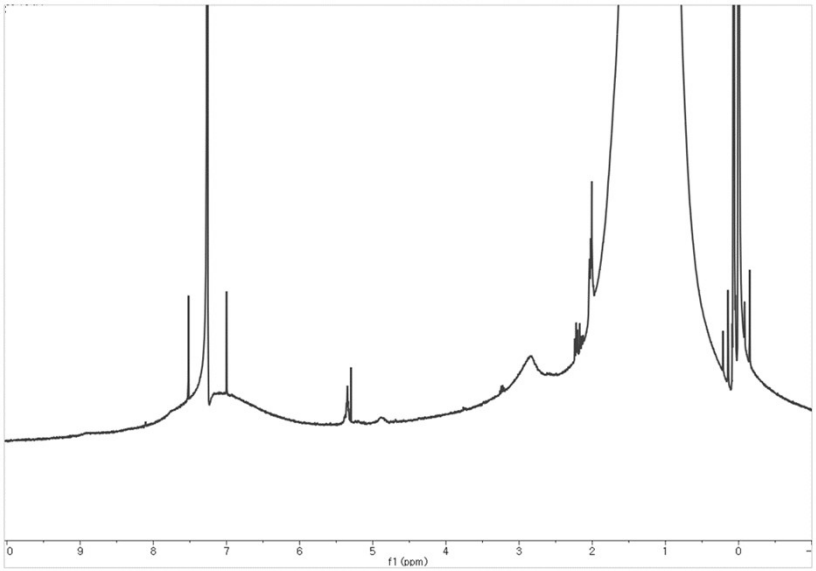

Fig. S1 ^{1}H NMR of PM6-Qx10.

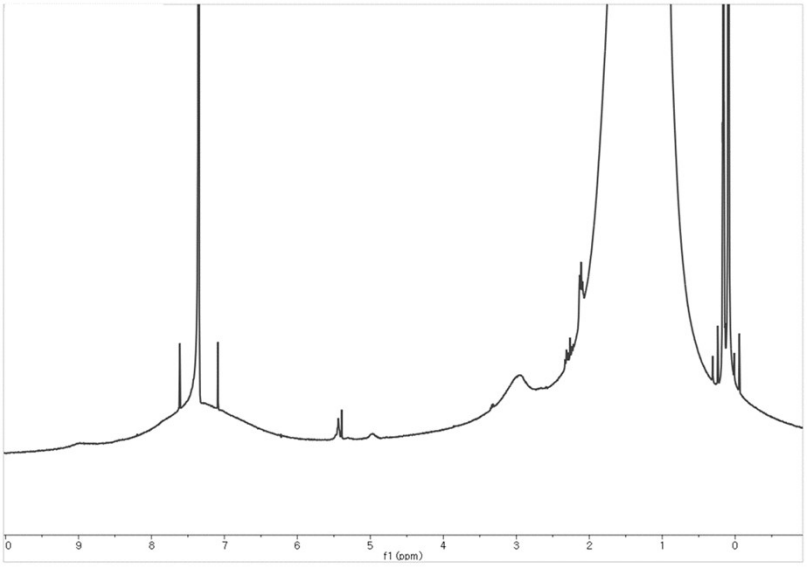

Fig. S2 ^{1}H NMR of PM6-Qx20.

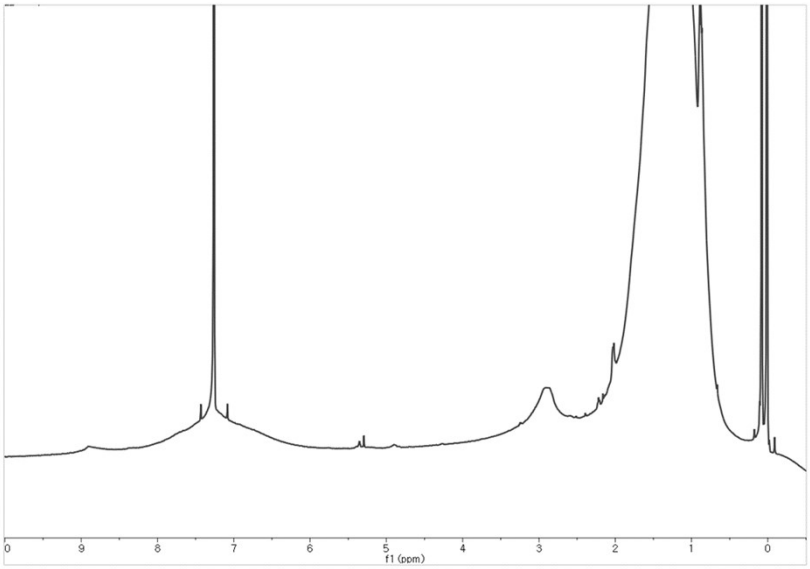

Fig. S3 ^{1}H NMR of PM6-Qx50.

Table S1 Optical and electrochemical properties of random polymers according to the loading time of the third component.

	λ_{sol}^{max} [nm]	λ_{film}^{max} [nm]	λ_{onset} [nm]	E_g^{opt} [eV]	E_{HOMO}^{CV} [eV]	E_{LUMO}^{CV} [eV]	M_n	PDI
PM6	614	617	678	1.83	–5.58	–3.15	38,153	3.22
PM6-Qx10	607	615	678	1.83	–5.58	–3.10	39,245	2.98
PM6-Qx20	576	576	676	1.83	–5.57	–3.07	39,267	2.81
PM6-Qx50	568	566	675	1.84	–5.55	–2.89	39,626	2.44

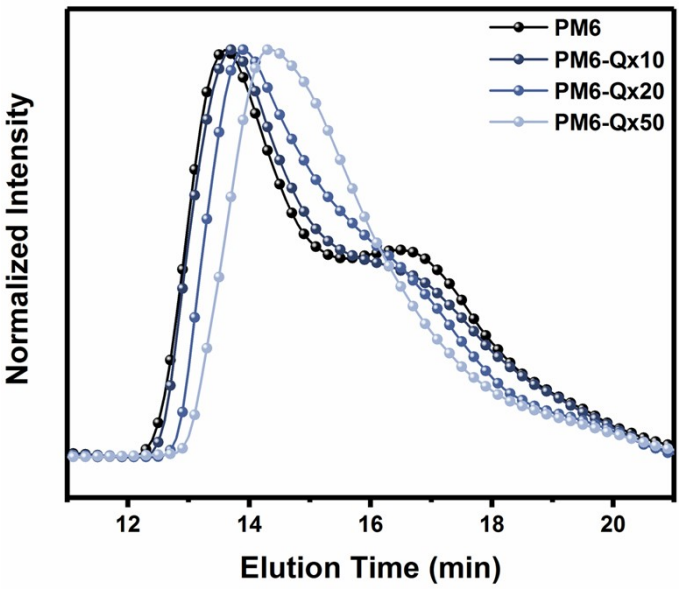

Fig. S4 GPC data of PM6, PM6-Qx10, PM6-Qx20, and PM6-Qx50.

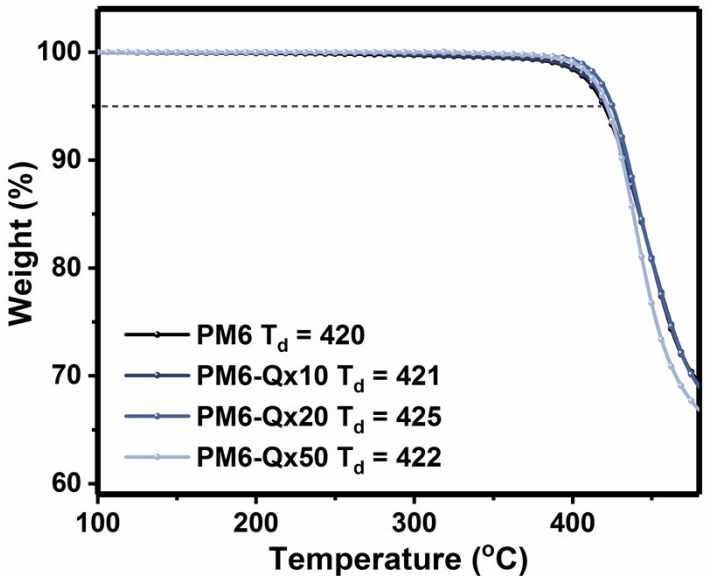

Fig. S5 TGA plots of PM6, PM6-Qx10, PM6-Qx20, and PM6-Qx50 at a scan rate of 10 °C min^{-1}.

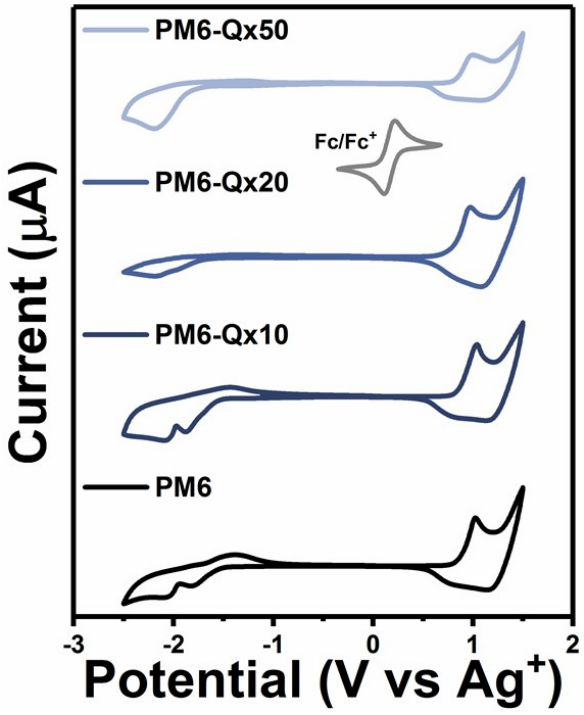

Fig. S6 CV profiles of PM6, PM6-Qx10, PM6-Qx20, and PM6-Qx50.

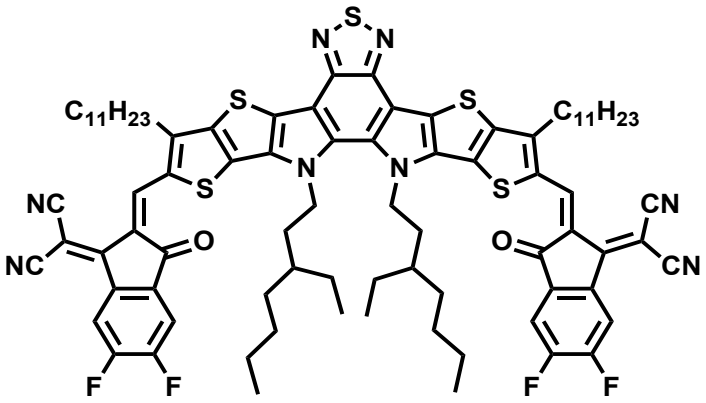

Fig. S7 The chemical structure of N3 acceptor.

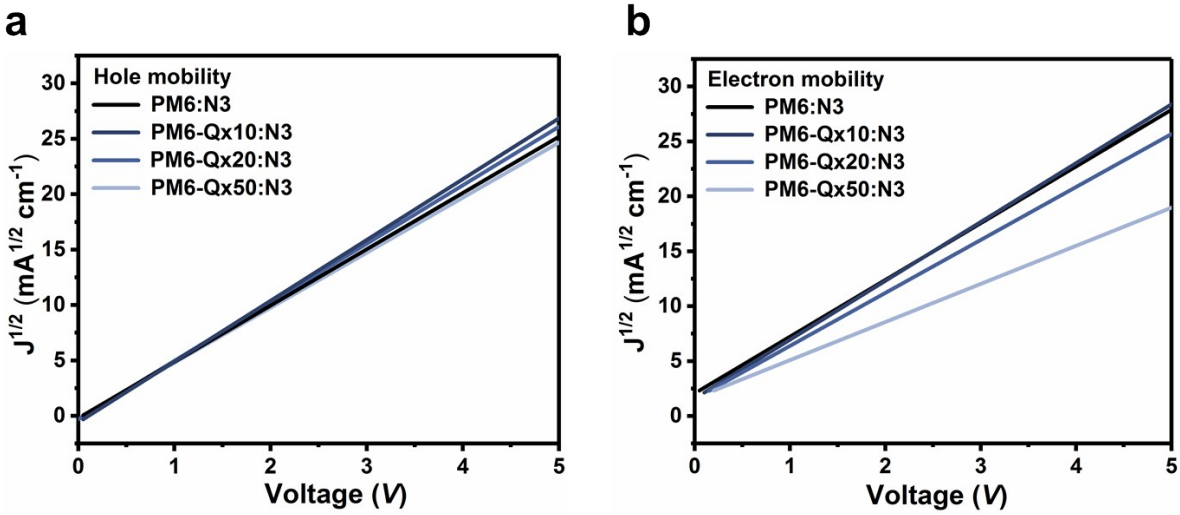

Fig. S8 SCLC plots of (a) hole- and (b) electron-only devices of blend films based on PM6, PM6-Qx10, PM6-Qx20, and PM6-Qx50.

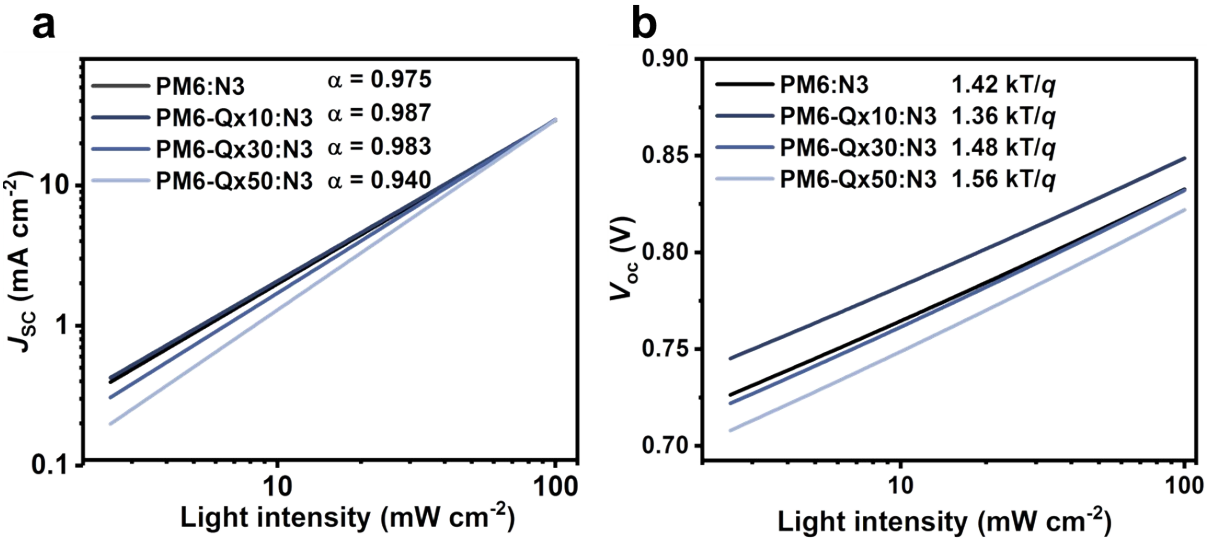

Fig. S9 (a) J_{sc} and (b) V_{oc} versus light intensity of the OSCs devices based on PM6, PM6-Qx10, PM6-Qx20, and PM6-Qx50.

Table S2. Summary of device parameters of PM6-Qx10:N3 blend films with different additive contents and annealing temperatures under illumination of AM 1.5G (100 mW cm^{-2}).

D/A ratio	Additive (%)	Annealing (°C)	V_{oc} [V]	J_{sc} [mA cm^{-2}]	FF [%]	PCE [%]
1:1.2	0.25	100	0.864	24.41	71.15	15.00
	0.5	100	0.861	25.13	73.42	15.90
	0.75	100	0.858	24.81	72.54	15.44
	0.5	80	0.864	25.13	72.88	15.82
		100	0.862	25.18	73.72	16.01
		120	0.858	25.02	71.89	15.43
		90	0.863	25.43	74.80	16.43

Table S3. Summary of device parameters of PM6-Qx10:N3 devices with different rotating speeds of the active layer under illumination of AM 1.5G (100 mW cm^{-2}).

rpm	V_{oc} [V]	J_{sc} [mA cm^{-2}]	FF [%]	PCE [%]
2100	0.857	25.04	73.08	15.68
2400	0.861	25.25	74.15	16.12
2700	0.863	25.43	74.80	16.43
3000	0.863	24.70	75.12	16.01

Table S4. Summary of device parameters of PM6-Qx10:N3 devices with different D/A ratios under illumination of AM 1.5G (100 mW cm^{-2}).

D/A ratio	V_{oc} [V]	J_{sc} [mA cm^{-2}]	FF [%]	PCE [%]
1:1.1	0.858	25.07	73.81	15.88
1:1.2	0.863	25.43	74.80	16.43
1:1.3	0.859	25.28	73.29	15.92

Table S5 Summary of charge mobilities on blend films based on PM6, PM6-Qx10, PM6-Qx20, and PM6-Qx50.

System	$\mu_{h(blend)}$ (10^{-4} cm^{-2} V^{-1} s^{-1})	$\mu_{e(blend)}$ (10^{-4} cm^{-2} V^{-1} s^{-1})	μ_h/μ_e
PM6:N3	4.82	4.09	1.18
PM6-Qx10:N3	5.81	5.11	1.14
PM6-Qx20:N3	4.79	3.90	1.23
PM6-Qx50:N3	3.09	2.31	1.34

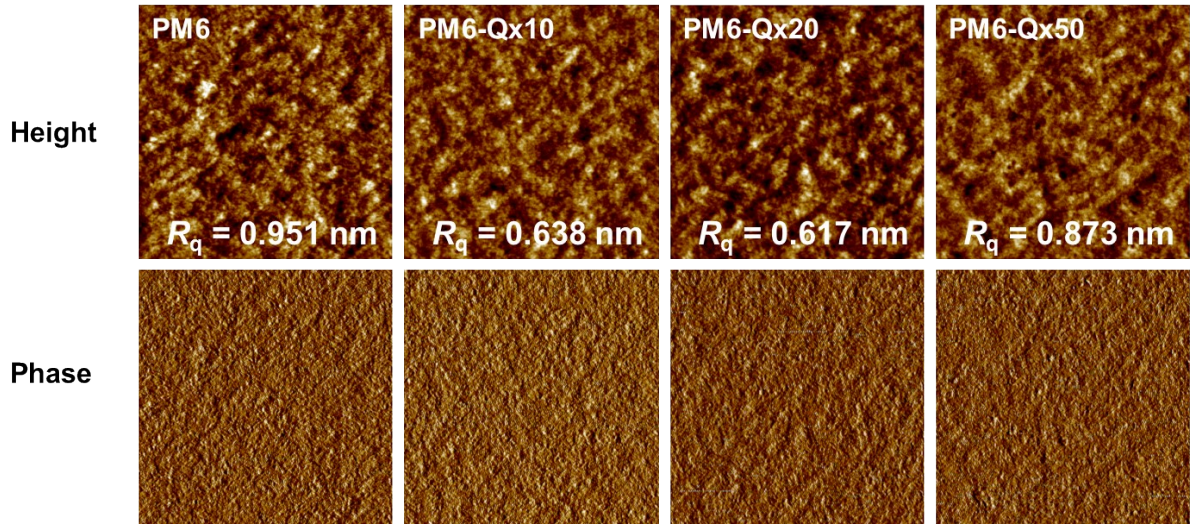

Fig. S10 Height AFM images of neat films with the corresponding RMS values (R_q).

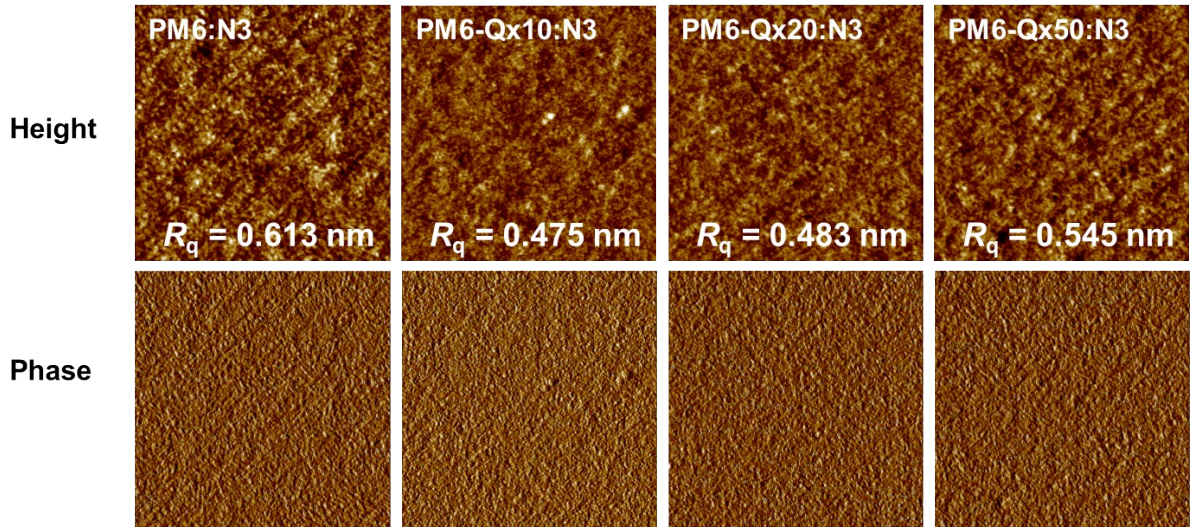

Fig. S11 Height AFM images of blend films with the corresponding RMS values (R_q).

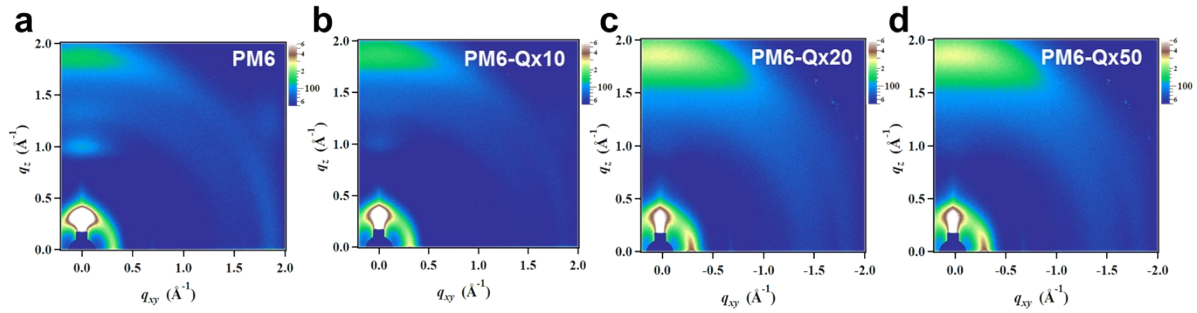

Fig. S12 (a–d) 2D GIWAX images of neat films based on the PM6 copolymer and PM6-Qx terpolymers.

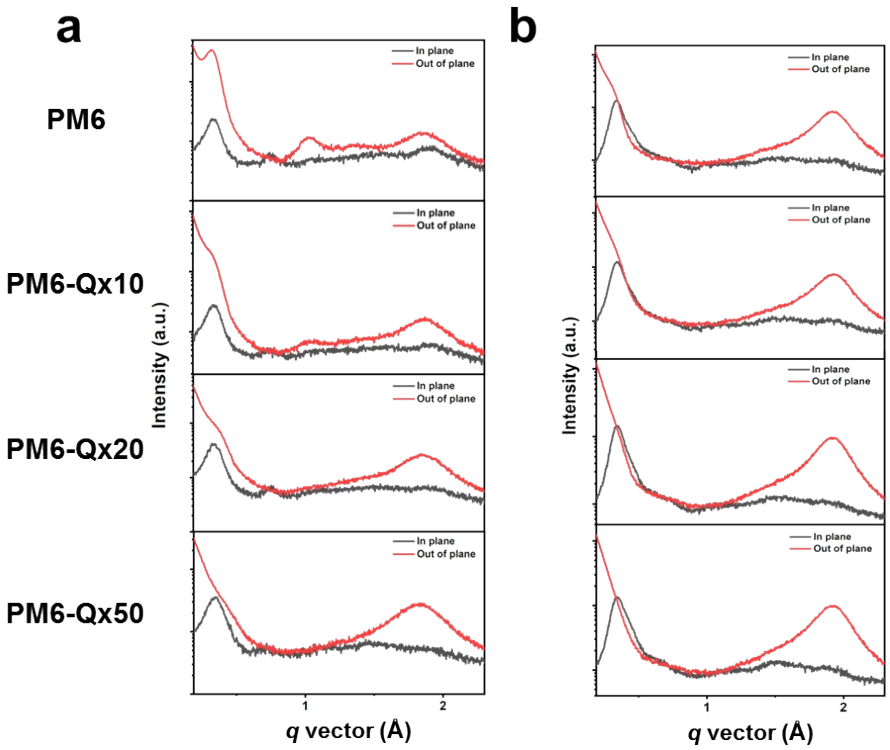

Fig. S13 Line cut profiles of (a) neat and (b) blend films based on of PM6, PM6-Qx10, PM6-Qx20, and PM6-Qx50.

Table S6 Lattice parameters in out-of-plane and in-plane direction for PM6 and PM6-Qx series-based neat films.

Systems	Out-of-Plane				In-Plane			
	π-π stacking cell axis (*010*)				Lamellar packing *(100)*			
	q (Å^{-1})	*d*-spacing (Å)	FWHM (Å^{-1})	Coherence length (Å)	*q* (Å^{-1})	*d*-spacing (Å)	FWHM (Å^{-1})	Coherence length (Å)
PM6	1.844	3.407	0.333	17.199	0.335	18.734	0.109	51.819
PM6-Qx10	1.851	3.394	0.294	19.483	0.336	18.673	0.111	51.006
PM6-Qx20	1.842	3.411	0.322	17.766	0.338	18.593	0.112	50.705
PM6-Qx50	1.815	3.462	0.344	16.619	0.341	17.425	0.143	39.649

Table S7 Lattice parameters in out-of-plane and in-plane direction for PM6 and PM6-Qx series:N3-based blend films.

Systems	Out-of-Plane				In-Plane			
	π-π stacking cell axis (*010*)				Lamellar packing *(100)*			
	q (Å^{-1})	*d*-spacing (Å)	FWHM (Å^{-1})	Coherence length (Å)	*q* (Å^{-1})	*d*-spacing (Å)	FWHM (Å^{-1})	Coherence length (Å)
PM6	1.923	3.267	0.226	25.401	0.343	18.322	0.083	85.682
PM6-Qx10	1.928	3.259	0.213	26.938	0.343	18.322	0.089	112.460
PM6-Qx20	1.922	3.269	0.223	25.456	0.342	18.361	0.090	120.742
PM6-Qx50	1.921	3.270	0.246	23.321	0.354	17.758	0.116	162.644

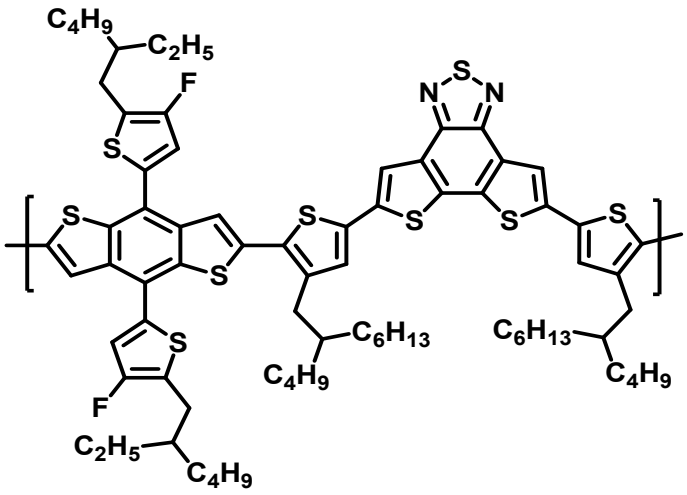

Fig. S14 The chemical structure of D18 polymer.

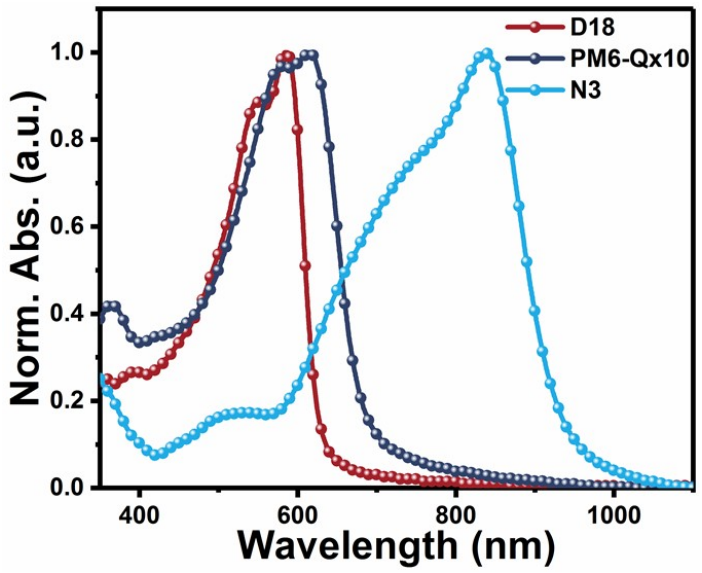

Fig. S15 Normalized absorption spectra of D18, PM6-Qx10, and N3.

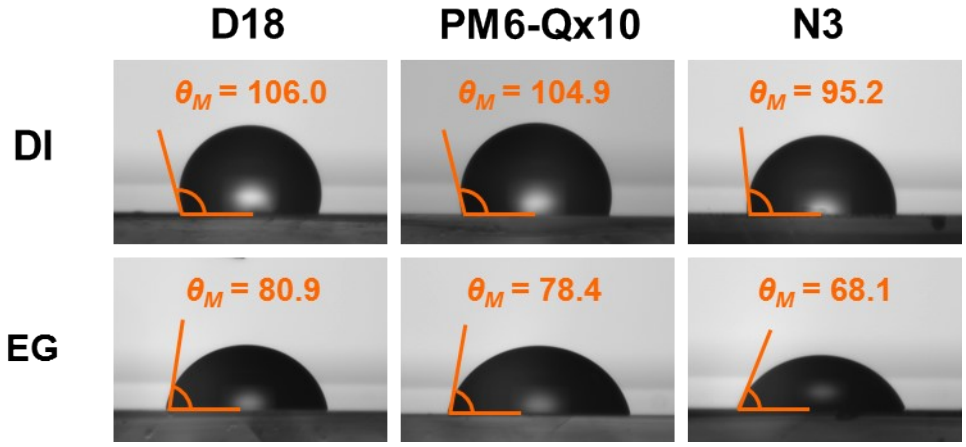

Fig. S16 Contact angle measurement images of the neat D18, PM6-Qx10, and N3 using DI and EG.

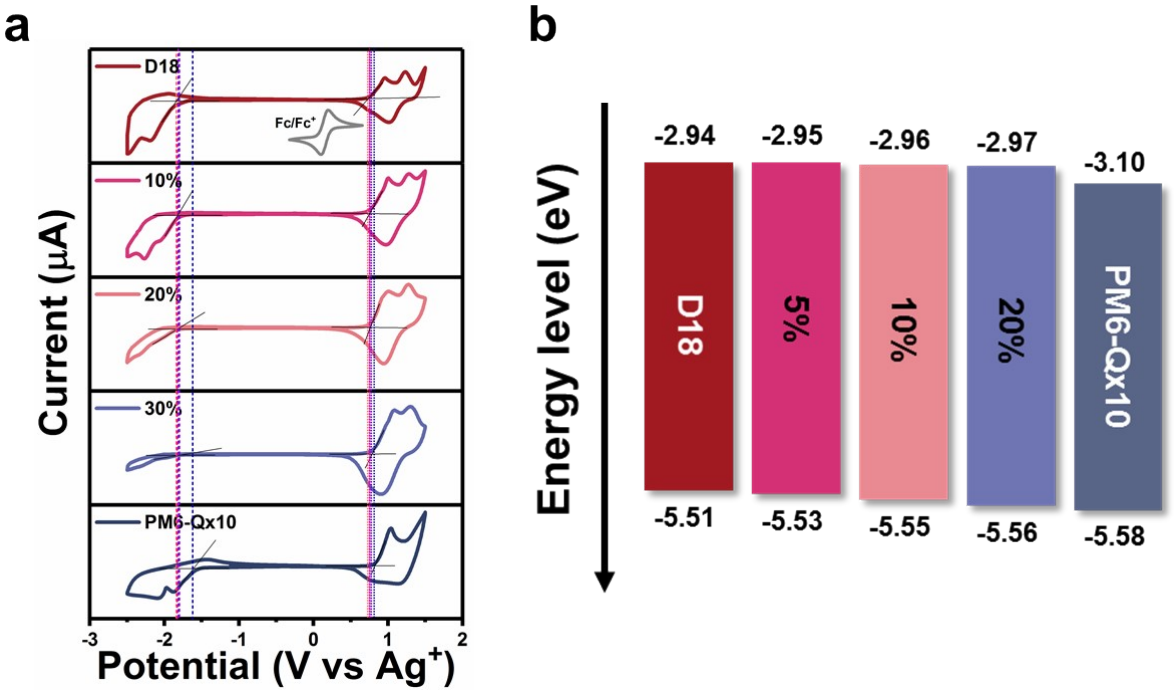

Fig. S17 (a) CV profiles and (b) energy level diagrams of PM6-Qx10:D18 alloy as a function of PM6-Qx10 content.

Table S8 Lattice parameters in out-of-plane and in-plane direction for PM6 and PM6-Qx series:N3-based blend films.

Systems	Contact angle		Surface Energy [mN m^{-1}]	Interfacial Energy [mN m^{-1}]	
	Θ_{DI} [°]	Θ_{EG} [°]		D18	PM6-Qx10
D18	106.0	80.9	21.19	-	0.0978
PM6-Qx10	104.9	78.4	22.79		-
N3	95.2	68.1	25.69	1.3855	1.6146

References

1 Y. Xu, Y. Cui, H. Yao, T. Zhang, J. Zhang, L. Ma, J. Wang, Z. Wei and J. Hou, *Adv. Mater.*, 2021, **33**, 2101090.

2 J. Yao, B. Qiu, Z. Zhang, L. Xue, R. Wang, C. Zhang, S. Chen, Q. Zhou, C. Sun, C. Yang, M. Xiao, L. Meng and Y. Li, *Nat. Commun.,* 2020, **11**, 2726.